# Study on flow and pressure fluctuation characteristics of two-way pumping system with super low head and large flow rate

# Study on flow and pressure fluctuation characteristics of two-way pumping system with super low head and large flow rate

**Weixuan Jiao, Li Cheng※, Can Luo, Di Zhang**

School of Hydraulic, Energy and power Engineering
Yangzhou University, Yangzhou, Jiangsu, P.R.China, 225009

E-mail: chengli@yzu.edu.cn

**Abstract.** The pumping station along the Yangtze River runs around the zero head all the year round, and the work flow rate deviates from the design condition, which is easy to cause hydraulic vibration, and seriously affects the safety of the unit. By using the CFD software, the numeric simulation of typical low head Two-way pumping system was made. The flow characteristics and pressure fluctuation characteristics of two-way flow channel with large flow rate are calculated and analysed. The calculated results are verified by model tests. The results show: Under the super low head condition, the flow pattern of the main flow area of the inlet and outlet channel is better, but the blind end of the inlet and outlet of the flow channel has larger reflux. The pressure fluctuation at the monitoring point of the impeller and guide vane has obvious periodic variation rule. Due to impeller rotation, the pressure fluctuation exists alternately in the impeller. Frequency domain graph display based on fast Fourier transform, the main frequency of each point at the outlet of the impeller are all blade passing frequency (BPF). The main frequency of impeller inlet and guide vane outlet was the multiples of BPF. The pressure fluctuation in the inlet and outlet channel is more complicated, the low frequency fluctuation dominates, and the fluctuation amplitude decreases greatly. The research results can provide reference for hydraulic vibration research of super low head pumping station along the Yangtze River.

## 1. Introduction

In the lakeside area along the Yangtze River, the super low head pump station is widely distributed. These pumping stations have played an irreplaceable role in the long-term flood control and disaster reduction work, and become an important infrastructure to ensure economic growth. However, due to the frequent changes of the Yangtze River water level, pumping station along the river often run to super low head condition, or even zero or negative head. Under this condition, the unit deviates from the design condition seriously. This can easily lead to abnormal water pressure fluctuation, which causes the strong vibration of the unit and seriously threatens the safety of the pumping station [1-4].

With the deepening of the reconstruction work of the small and medium pump stations in Jiangsu, the hydraulic resonance and the prevention and control technology under the super low head of the pumping station along the Yangtze River are extremely urgent. Wang [5] used unsteady flow analysis

theory and large eddy simulation to study the results of water pressure fluctuation in axial flow pump under different working conditions. Qian[6] used SST k- ω turbulence model to simulate Three-dimensional unsteady turbulent of the pump turbine model, the research shows that the vortex belt shape and direction of rotation has great influence on the unit pressure fluctuation. In order to study the pressure fluctuation characteristics of axial flow pump under different flow conditions, Zhang[7] arranged a number of pressure fluctuation monitoring points on the outer wall of axial pump impeller and guide vane to conduct dynamic measurement, and the pressure fluctuation at different locations inside the axial flow pump was revealed. Combining with the new pumping station of South to North Water Transfer Project, Zheng [8] studied the characteristics of pressure fluctuation in different blades under the angle and head of the downstream axial pump by physical model test. Liu [9] proposed a new type of curve diffusion water structure and the design scheme of inlet guide pier for the low efficiency of the traditional box type two-way flow channel pump, and the problem of water swirl in the inlet channel is easy to be produced. Through numerical simulation, it is verified that the new design improves the efficiency of the pump unit and eliminates the underwater vortex, which can effectively guarantee the economy and safety of the operation of the pump unit.

There are many researches on the pressure fluctuation of axial flow pump and two-way channel design optimization, but there are few studies on the flow characteristics and pressure fluctuation characteristics of pump station under super low head conditions. Therefore, this paper used CFD (Computational Fluid Dynamics) [10] to calculate and analyse the flow characteristics under the condition of super low head condition for the typical two-way channel pump device along the Yangtze River. Through the calculation of unsteady pressure fluctuation characteristics, we can provide a reference for the study of the hydraulic vibration problem of super river pumping station with low head.

## 2. Numerical simulation

### *2.1. Calculation model*

The calculation model is a super low head two-way channel pumping station along the Yangtze River (Figure 1). The design flow of pumping station is 20 $m^3/s$. The diameter of pump impeller is 2.50m. The speed n=150r/min, the blade number is 3, and the guide vane number is 7. The main motor is synchronous motor, and the single machine power is 1000Kw. There are 4 steel gates in the inlet and outlet channels of each pump unit. The direction of pumping or draining can be controlled through the gate. The net head of the condition of drainage of the two-way pumping station is 2.61m, and the net head of the condition of water diversion is 1.89m. The calculation model of the pumping station mainly includes the inlet channel, the impeller, the guide vane and the outlet channel (Figure 2).

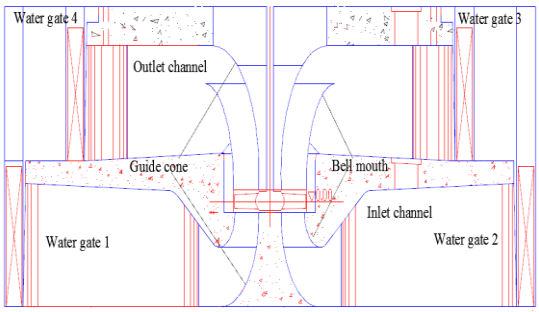


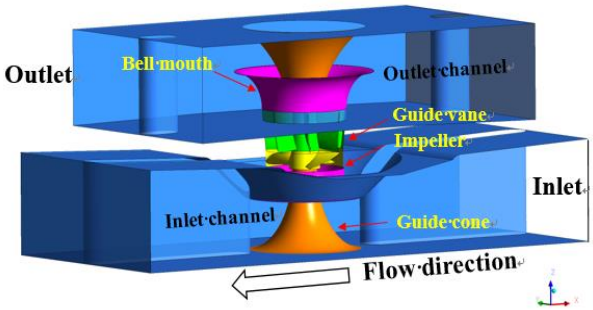


**Figure 1.** Two-way Channel Vertical Pumping System. **Figure 2.** Three dimensional model of Two-way Channel Vertical Pumping System.

### *2.2. Calculation Method and mesh generation*

This paper was based on the continuity equations of incompressible fluid and the time averaged Reynolds equation (RANS equation). The large commercial software CFD was used for numerical simulation. The RNG k-ε model was used in the three-dimensional steady and unsteady calculation. Several studies [11-13] have revealed that the RNG *k-ε* model can predict the swirling flow and vortex flow very well, and has good applicability in the flow field of the axial flow pump. The error of head

and efficiency is less than 3%, which can meet the requirements of engineering application. Because this paper studied incompressible fluid, the heat exchange was basically ignored. Due to the energy conservation equation was not considered, the effect was not considered in the calculation process.

The Mesh and TurboGrid in ANSYS software were used to mesh the inlet and outlet channel, the extended section, the guide vane and impeller respectively. The grid is a mixed grid. Due to the complex shape of the inlet and outlet channels, the hexahedral grids were used in most fields, and the unstructured tetrahedral meshes were used in a few parts. In order to ensure the accuracy of the calculation, the mesh density of the impeller and the guide vane was densified when the grid was divided. As different turbulence models require different y+ values of the grid, the RNG k- ε model requires the y+ value to be guaranteed to be between 30~100[14-15].

In order to verify the reasonableness of the mesh generation, the inlet channel grid independent analysis was carried out (Figure 3a). The analysis of grid independence shows that when the grid number of the intake sump reaches 2,480,000, the head is 2.57m, and the calculation results are accurate and the number of grids is reasonable. The total grid is 8,220,000. Figure 3 is a schematic diagram of Grid independence and Grid classification.

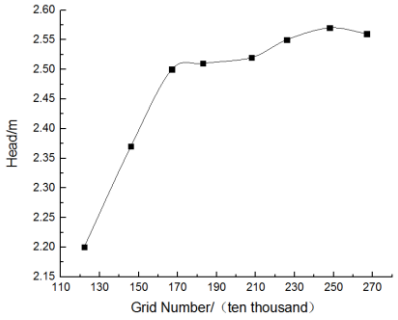


（a）Grid independence

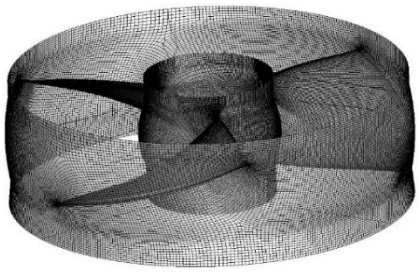

（b）Impeller Grid

**Figure 3.** Grid independence and Grid generation.

*2.3. Calculation parameters and boundary conditions*

Pump impeller diameter D=2500mm, speed n=150r/min. In order to study the characteristics of pressure fluctuation under super low head and large flow rate condition, the regular large flow rate (Q=28 m³/s) as condition was calculated and analysed.

The calculated region includes the inlet channel and the extension, the impeller, the guide vane, the outlet channel and the extension. The boundary conditions are set as follows: The inlet boundary is set up on the extension section of the inlet channel, and the quality inlet condition is adopted and the mass flow on the inlet boundary is given. The outlet boundary is far away from the outlet channel, and the entrance pressure condition is adopted, and the average static pressure is 1atm.

The non-slip condition ($u = v = w = 0$) is defined at the side wall of the solid, and the wall function is used in the near wall area. The surface of the blade is set as a moving wall. For pumping stations, there are rotating impeller, stationary guide vane and inlet and outlet flow channels. The dynamic and static interfaces are set between the inlet channel, the impeller and the guide blade. The steady calculation uses the multi reference frame model to deal with the dynamic and static interface. The Transient Rotor Stator interface is used in the unsteady calculation. The calculation precision is 1 x $10^{-4}$. In the unsteady calculation, the time step is 1/40[16-18] of the impeller rotation period, and the rotation period is 0.4s, and the sampling time takes 8 impeller rotation cycles [19].

## 3. Test Verification

The energy performance test of the two-way flow channel pump system was completed on the pump model test-bed of Jiangsu University. The whole test-bed consists of the inlet and outlet water tank, the measured pump device, the pressurizer, the electromagnetic flowmeter, the booster pump, the differential gauge, the gate valve and so on. The design and arrangement of the test-bed are reasonable

and the installation and adjustment are convenient. The system runs steadily and has good repeatability, and the comprehensive error of its efficiency measurement is ±0.79%. The two-way flow channel pump test bench system is shown in Figure 4.

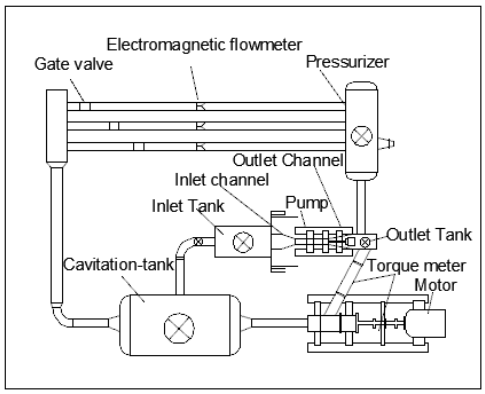


**Figure 4.** Test bench of axial-flow pump.

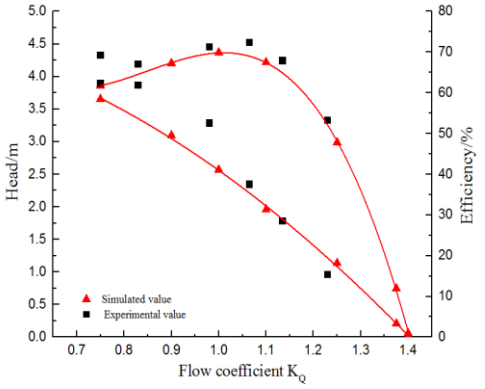


**Figure 5.** Comparison of hydraulic performance between simulated value and experimental value.

As shown in Figure 5, the performance data of the pump system measured by the test-bed are converted according to the SL140-2006《Code for model pump and its installation acceptance tests》prototype pump performance conversion method. The conversion formula of the model pump characteristic of the prototype pump numerical simulation result is as follows:

$$\frac{Q_p}{Q_m} = \frac{n_p D_p^3}{n_m D_m^3} \qquad \frac{H_p}{H_m} = \frac{n_p^2 D_p^2}{n_m^2 D_m^2}$$

Note: $Q_p$、$Q_m$—Prototype pump and model pump flow, $H_p$、$H_m$—Prototype pump and model pump head, $n_p$、$n_m$—Prototype pump and model pump speed, $D_p$、$D_m$—Prototype pump and model pump impeller diameter. ( $n_p$= 150r/min, $n_m$=1275r/min, $D_p$ =2500mm, $D_m$=300mm.)

The performance data of the prototype pump were compared with the numerical simulation, and the overall trend is similar. However, when the flow coefficient is $K_Q$<1, the difference between them is more obvious. When $K_Q$>1, the two values are similar and the error is smaller. The flow coefficient in the figure is the ratio of the calculated flow to the design flow. Because the prototype pumping station often runs under the condition of super low head, such as the zero head or even the lift head, when the calculated flow reaches 1.4 times the design flow, the device head is 0.01m, so it is calculated and analysed as an super low lift condition, and the data is reliable.

## 4. Calculation results

### *4.1. Flow characteristic*

Figure 6 is the streamline in the pump unit. It is known from the diagram that the flow pattern in the inlet channel is better and the flow of the main flow area is relatively smooth, but there is a larger reflux area in the blind end of the flow channel, and the flow pattern is rather disorganized. Because the blind end of the inlet channel is relatively long, the flow velocity is lower and the backflow intensity of the blind end is relatively small, which has little influence on the water flow and hydraulic loss at the inlet section of the pump. The flow pattern in the outlet channel is complex, and the f streamline is swinging larger. This is due to the large amount of residual circulation at the outlet of the impeller and the secondary back-flow caused by the change of the direction of the flow of 90 degrees. The water flow in the outlet channel is influenced by the residual circulation of the outlet flow of the guide vane, and the streamlines are spiral and offset to the top wall of the outlet channel. The blind end of the outlet channel is shorter, the diffusion angle of the guide vane is larger and the reflux intensity is larger, which leads to the increase of hydraulic loss in the outlet channel.

Figure 7 is the surface static pressure distribution. It can be seen from the diagram that there is a small area of high pressure due to the impact of the flow of water on the inlet of the blade. Under the

large flow condition, the high-pressure zone of the blade is shifted to the suction surface, and the static pressure at the inlet of the suction surface is greater than that of the pressure surface.

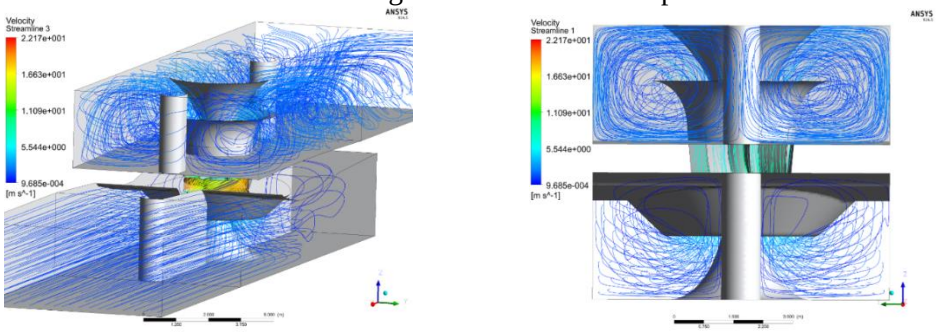


**Figure 6.** Streamline of pumping system.

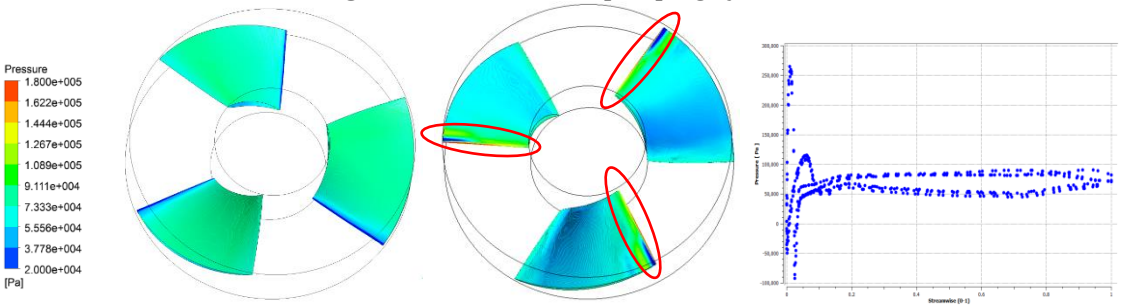


(a)Pressure surface （b）Suction surface （c）Span=0.95

**Figure 7.** Static pressure distribution on blade surface.

*4.2. Pressure fluctuation characteristic*

*4.2.1. Arrangement of monitoring points*

In order to analyse the pressure fluctuation of each part of the pump, sixteen pressure fluctuation monitoring points of pressure fluctuation were set up in the calculation model (Figure 8). Among them, Monitoring points M1, M2 and M3 were set up at the impeller inlet along the direction of the wheel hub to the wheel flange. Monitoring points M4, M5 and M6 were arranged in turn at the impeller outlet. Monitoring points M10, M11, and M12 were set at the intake bell mouth of the inlet channel. Monitoring points M13, M14, M15 and M16 are set at the floor and top of the outlet channel.

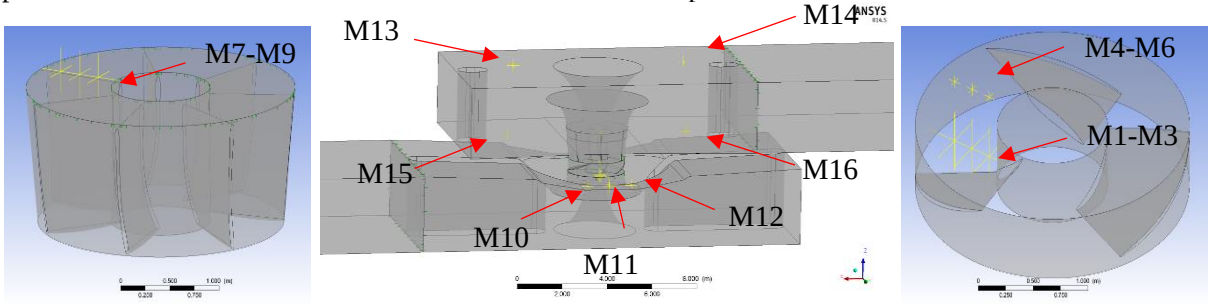


（a）Guide Vane （b）Inlet and Outlet Channel （c）Impeller

**Figure 8.** Location of monitoring points.

*4.2.2. Time domain analysis*

8 times impeller rotation period was used as sampling time to analyse the pressure fluctuation of the axial flow pump. In order to analyse the pressure fluctuation, the pressure fluctuation coefficient $C_p$ was introduced.

$$C_p = \frac{p-\bar{p}}{0.5\rho u^2} \quad (1)$$

Note: $p$——Instantaneous pressure， Pa, $\bar{p}$——Time-average pressure， Pa, $\rho$——Water density， kg/m$^3$, u——Circumferential velocity of the impeller， m/s

The rotation period number is defined N=t/T, and the t in the formula is the acquisition time for any point signal, and the T is the 1 week rotation time of the impeller. In order to show the time domain rule of the fluctuation clearly, the time domain diagram of this paper is the pressure fluctuation data of 4 weeks.

Figure 9 is the time domain diagram of pressure fluctuation of each point M1 to M16. From the graph, we can see that the pressure fluctuation of the inlet and outlet of the impeller and the outlet of guide vane have obvious periodic change. The pressure fluctuation is not regular in the inlet and outlet channel due to the reflux and diffusion of water.

The periodic law of pressure fluctuation of monitoring points at impeller inlet is good (Figure. 9a). Due to the influence of impeller rotation, there are 1 obvious wave crest and wave troughs in 1 impeller rotation periods. In the flow channel of the impeller, the pressure of the monitoring point at the inlet of the impeller is alternately pulsating due to the rotating effect of the impeller.

The pressure fluctuation waveform at the outlet of the impeller is regular (Figure. 9b). Due to the influence of blade number, there are 3 obvious wave crests and wave troughs in the 1 impeller rotation periods. However, due to the existence of the internal reflux or the blade tip vortex in the impeller, the waveform appears two wave peaks.

The pressure fluctuation of the monitoring point at the guide blade is still influenced by the rotation of the impeller and the number of the blades (Figure 9c). As the flow of the guide vane at the outlet of the two-way channel is disordered, and the reflux in the outlet channel is larger, the amplitude of the pressure fluctuation is on the rise.

Due to the change of inflow angle of impeller inlet, the time domain diagram of pressure fluctuation at the bell mouth of the inlet channel is disorderly and there is no obvious law (Figure 9d). Due to the bad flow phenomena such as local reflux at the inlet of the impeller, the amplitude is on the rise.

As the water flows out of the guide vane, it still has a certain velocity circulation. The flow of the bell mouth is uneven. Large reflux appears in the blind end of the outlet channel. The complexity of the random components of pressure fluctuation is more complex, the waveform is irregular, and the flow at the bottom of the outlet is more chaotic, and the amplitude is increasing (Figure 9e).

The amplitude of the monitoring points is compared. The amplitude of the monitoring points at the inlet and outlet of the impeller is significantly higher than that at the outlet of the guide vane and the inlet and outlet channels, and the amplitude of the monitoring points at the outlet of the impeller is higher.

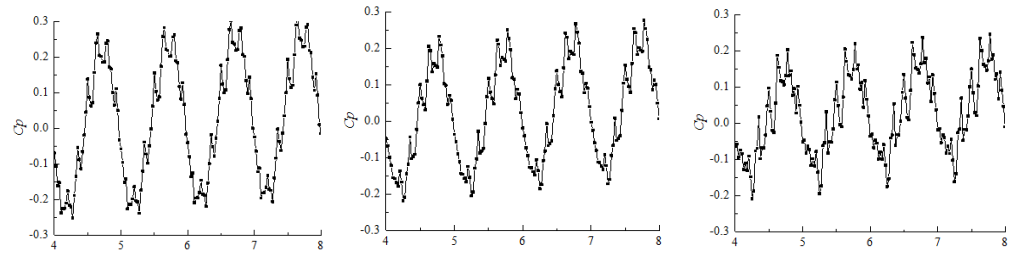


（a）Inlet of impeller

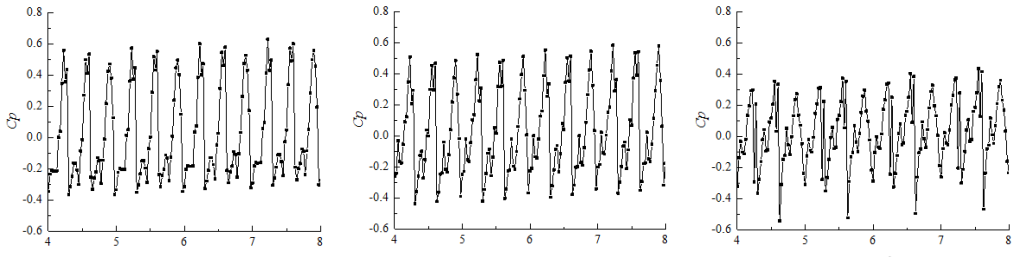

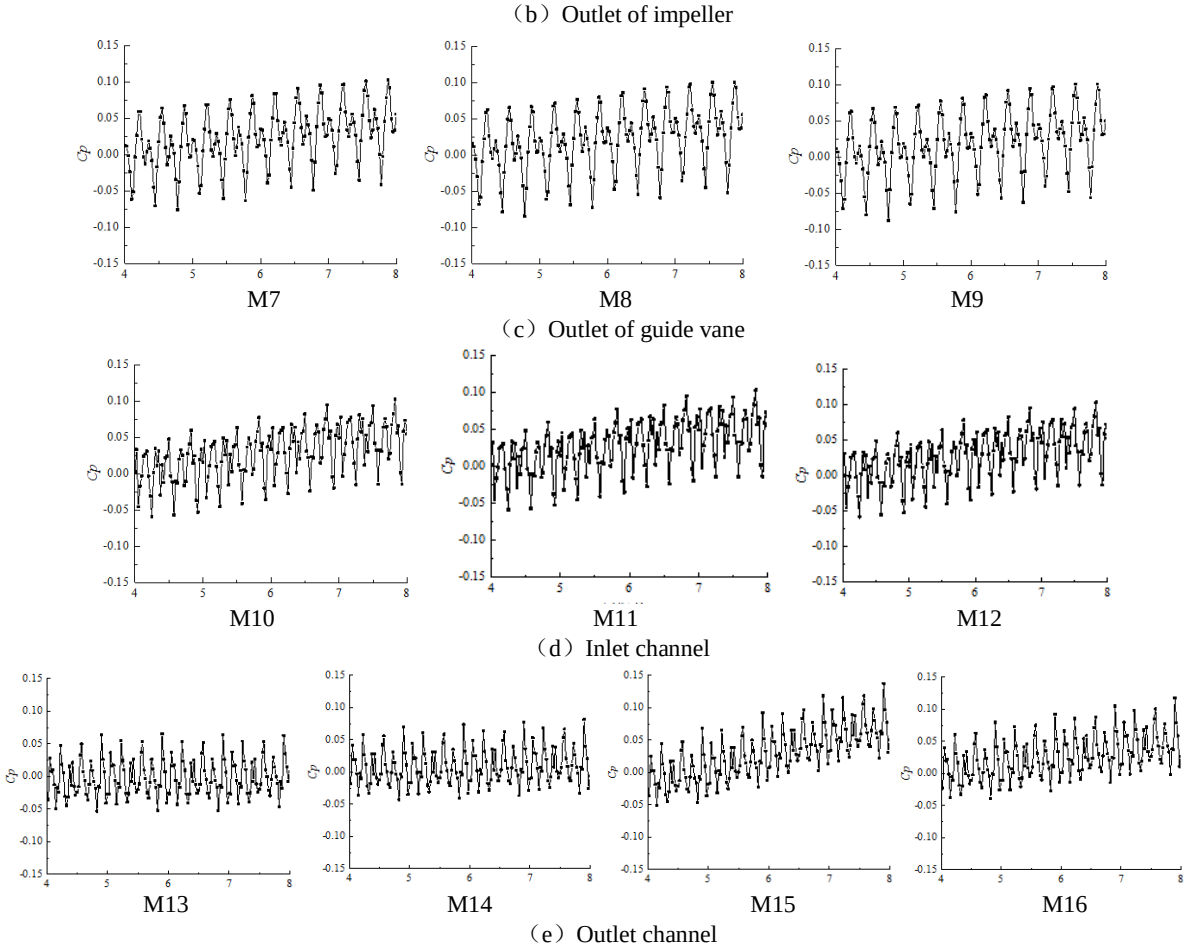


**Figure 9.** Time-domain distributions of pressure fluctuation at different monitoring points.

*4.2.3. Frequency domain analysis*

In order to analyse the law of the spectrum, the fast Fourier transform of the calculated pressure fluctuation data is carried out, and the frequency domain diagram of the pressure fluctuation is obtained. In order to facilitate analysis, the frequency is represented by the frequency multiplier. Definition of the formula of frequency multiplier $N_F$

$$N_F = \frac{60F}{n} \tag{2}$$

Note: $F$——The actual frequency after the fast Fourier transformation $n$——Rotating speed

Using pressure difference to represent the amplitude of pressure in a spectrum diagram. Pressure difference $P^*$

$$P^* = P - \bar{P} \tag{3}$$

Note: $P$ ——Instantaneous pressure，kPa, $\bar{P}$ ——Average pressure，kPa

Figure 10 is the frequency domain diagram of pressure fluctuation of each point M1 to M16. From the graph, we can see that the main frequency of the pressure fluctuation of the monitoring points at the impeller inlet is the impeller rotation frequency, and the main frequency of the pressure fluctuation of the monitoring points at the outlet is the blade passing frequency (BPF). At the same time, when the frequency of the monitoring points at the impeller is 6 times as high as the rotational frequency, the high wave peak appears. Especially at the impeller outlet, the secondary frequency is 6 times as high as the rotational frequency. In the frequency domain diagram of pressure fluctuation of the monitoring points at the impeller inlet and outlet, when the frequency reaches 7 times as high as the rotational frequency, there is a higher amplitude. Therefore, the guide vane also affects the pressure fluctuation of the monitoring points at the impeller.

Compared with the amplitude of main frequency of the three monitoring points at the impeller inlet, it is found that the maximum amplitude of main frequency appears at the edge of the wheel. (Figure. 10a) The amplitude of pressure fluctuation gradually decreases along the direction of the wheel flange to the wheel hub. The amplitude of main frequency of M3 is 2.122kPa, which is 1.27 times of M2 point and 1.72 times of M1 point.

The amplitude of pressure fluctuation at the impeller outlet is opposite to that at the inlet (Figure. 10b), the amplitude of main frequency of the monitoring point at the hub is the largest, and gradually decreases along the hub to the wheel flange. The amplitude of main frequency of M4 point is 3.459kPa, which is 1.13 times of M5 point and 1.68 times of M6 point.

The variation of the main frequency of the pressure fluctuation at the guide vane outlet is irregular (Figure 10C). There are 2 monitoring points in the 3 monitoring points at the guide vanes, the main frequency is BPF, and the 1 monitoring point is 6 times the main frequency. The effect of the number of guide vane blades on the pressure fluctuation can be seen at 7 times the frequency of the monitoring point at the guide vane. Moreover, the amplitude of the main frequency is similar to that of the secondary frequency, and the low frequency fluctuation is dominant. Because the impeller rotation affects the pressure fluctuation at the monitoring point of the guide vane, and the main frequency of the monitoring points at the guide vane is the blade passing frequency. The amplitude of pressure pulsation at the outlet of the guide vane is similar, and the change is similar. The main frequency and amplitude of the pressure fluctuation at the flange point is the largest, and decreases gradually along the wheel flange to the hub.

The pressure fluctuation in the inlet channel is more complicated (Figure.10d). The main frequency of the monitoring points is 6 times the main frequency, and the secondary main frequency is 1/8 times that of the impeller rotation frequency. The influence of the blade on the pressure fluctuation of the monitoring point is not obvious, and the amplitude of the pulsation is greatly reduced.

The main frequency of the monitoring points in the outlet channel has no obvious rule (Figure.10e), but the amplitude is similar. The main frequency of M14 point has a low frequency multiplier. The low frequency pulsation is dominant, and the impeller rotation almost has no effect on the pressure fluctuation of the outlet channel.

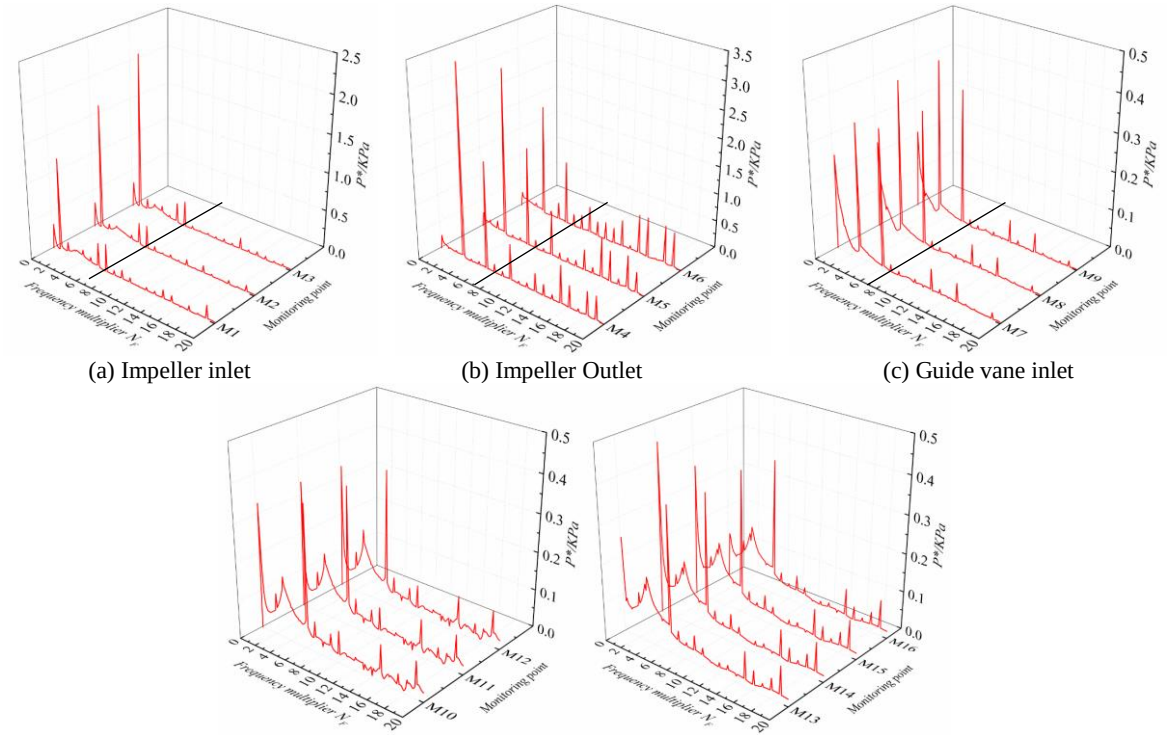


(a) Impeller inlet (b) Impeller Outlet (c) Guide vane inlet

(e) Inlet Channel (e) Outlet Channel

**Figure 10.** Frequency-domain distribution of pressure fluctuation at different monitoring points.

## 5. Conclusion

In this paper, numerical simulation combined with test verification method is used to study the flow and pressure fluctuation characteristics of the Two-way pumping system, and the following conclusions are obtained:

- There is a reflux zone in the blind end of the inlet and outlet channel. Among them, the flow rate of the blind end of the outlet channel is greater, and the hydraulic loss is greater. At the same time, the pressure distribution on the impeller surface is uneven, and the static pressure in the part of the suction surface near the inlet edge of the impeller is larger than the corresponding area of the pressure surface. The reflux of the outlet channel is easy to form whirlpool, reducing the overall efficiency of the pumping station and bringing the vibration and noise.
- According to the characteristics of pressure fluctuation, the pressure fluctuation of the monitoring point at the guide vane and the impeller is more regular, and there is no harmful frequency. The inlet and outlet flow path is less affected by impeller rotation, and the pressure fluctuation is regular. Low frequency fluctuation dominates, pressure fluctuation is complex, but the overall amplitude is small.
- The model test proves that the numerical simulation data is reliable under the condition of large flow rate.

**Nomenclature**

| | |
|---|---|
| $D_p$ | Prototype pump impeller diameter |
| $D_m$ | Model pump impeller diameter |
| $F$ | The actual frequency after the fast Fourier |
| $H_p$ | Prototype pump |
| $H_m$ | Model pump head, |
| $n$ | Rotating speed |
| $n_p$ | Prototype pump rotating speed |
| $n_m$ | Model pump rotating speed |
| $P*$ | Pressure difference |
| $p$ | Instantaneous pressure |
| $\bar{p}$ | Time-average pressure |
| $\rho$ | Water density |
| $Q_p$ | Prototype pump flow rate |
| $Q_m$ | Model pump flow rate |
| u | Circumferential velocity of the impeller |

## 6. Acknowledgments

This work was financially supported by National Natural Science Foundation of China (Grant No. 51779214, "The 12th Five-year" Key Project of National Science and Technology Support Plan(2015BAD20B01), The Young academic Leaders in Blue Project of Jiangsu, Peak plan six talents in Jiangsu province, Water conservancy science and technology project of Jiangsu Province (No. 2016035), A Project Funded by the Priority Academic Program Development of Jiangsu Higher Education Institutions(PAPD), Postgraduate Research & Practice Innovation Program of Jiangsu Province, The national college students' science and technology innovation project.

## References

[1] Y Zheng, Y J Chen, R Zhang, X F Ge and A Sun 2017 *J.* Analysis on unsteady stall flow characteristics of axial-flow pump *Transactions of the Chinese Society for Agricultural Machinery* **48** 127-35

[2] Atia E. Khalifa and Ben-Mansour R 2011 *J.* Study of pressure fluctuations and induced vibration at blade-passing frequencies of a double volute pump *Transactions of the CSAE* **36** 1333-45

[3] W D Shi, H F Leng, D S Zhang, F Long and H Zhang 2011 *J.* Performance prediction and experiment for pressure fluctuation of interior flow in axial-flow pump *Transactions of the Chinese Society for Agricultural Machinery* **42** 44－8
[4] S L Wang, L TAN and Y C Wang 2013 *J.* Characteristics of transient cavitation flow and pressure fluctuation for a centrifugal pump *Journal of Vibration and Shock* **32** 168-73
[5] F J Wang, L Zhang and Z M Zhang 2007 *J.* Analysis on pressure fluctuation of unsteady flow in axial-flow pump *Journal of Hydraulic Engineering* **38** 1003-9
[6] Z D Qian, J Lu, Z W Guo and J J Zhang 2016 *J.* Characteristics of pressure fluctuation in pump-turbine under turbine mode *JDIME* **34** 672-8
[7] D S Zhang, H Y Wang, W D Shi, D Z Pan and P P Shao 2014 *J.* Experimental Investigation of pressure fluctuation with multiple flow rates in scaled axial flow pump *Transactions of the Chinese Society for Agricultural Machinery* **45** 139-45
[8] Y Zheng, J Liu, D Q Zhou, Y T Mao and M Q Liu 2010 *J.* Pressure fluctuation of model test in large-size axial-flow pump *Journal of Drainage and Irrigation Machinery Engineering* **28** 51-5
[9] C Liu, Y Jin, J R Zhou, F P Tang, C M Hao and J Han 2011 *J.* Study of internal flow in cube-type bidirectional passages of axial-flow pump system by numerical simulation and experiment *Journal of Hydroelectric Engineering* **30** 192-8
[10] X X Jiang, L L Wang, Y Zheng L Li and R T Zhang 2007 *J.* Study on hydraulic characteristics of low lift head pumping station *Advances in Science and Technology of Water resources* **27** 10-13
[11] D S Zhang, W D Shi, B Chen and X F Guan 2010 *J.* Unsteady flow analysis and experimental investigation of axial-flow pump *Journal of Hydrodynamics* **22** 35-43
[12] Yang G 2016 RNG k-ε pump turbine working condition of numerical simulation and optimization of the model *C. Int. Conf. on Intelligent Computing.* Springer International Publishing 684-93.
[13] D S Zhang, W D Shi, H Zhang, J Yao and X F Guan 2012 *J.* Application of different turbulence models for predicting performance of axial flow pump *Transactions of the CSAE* **28** 66-71
[14] Z Dan, F J Wang, R Tao and Y K Hou 2016 *J.* Research for impacts of boundary layer grid sc -ale on flow field simulation results in pumping station *Journal of Hydraulic Engineering* **47** 139-49
[15] J Tu, G H Yeoh, and Liu C 2012 *J.* Computational Fluid Dynamics: A Practical Approach *Artificial Organs* **33** 727-32
[16] Z F Yao, F J Wang, R F Xiao, H J Yan, Z Q Liu and M Wang 2010 *J.* Key issues in pressure fluctuation experiments for centrifugal pumps *Journal of Drainage and Irrigation Machinery Engineering* **28** 219－23
[17] W D Shi, J Yao and D S Zhang 2013 *J.* Influence of sampling frequency and time on pressure fluctuation characteristics of axial-flow pump *Journal of Drainage and Irrigation Machinery Engineering* **31** 190-4
[18] F Shi and Tsukamoto H 2001 *J.* Numerical study of pressure fluctuations caused by impeller-diffuser interaction in a diffuser pump stage *Journal of Fluids Engineering* **123** 466-74
[19] F J Wang, L Zhang, Y J Li and Z M Zhang 2008 *J.* Some Key Issues of Unsteady Turbulent Numerical Simulation in Axial-flow Pump *Chinese Journal of Mechanical Engineering***44** 73-7
[20] W Wang, J Pei, S Q Yuan and T Y Yin 2018 *J.* Experimental Investigation on Clocking Effect of Vaned Diffuser on Performance Characteristics and Pressure Pulsations in a Centrifugal Pump *Experimental Thermal & Fluid Science* **90**
[21] X Q Jia, B L Cui, Z C Zhu and Y L Zhang 2018 *J.* Numerical Investigation of Pressure Distrib -ution in a Low Specific Speed Centrifugal Pump *Journal of Thermal Science* **27** 25-33
[22] L J Shi, F P Tang, R S Xie and W P Zhang 2017 *J.* Numerical and experimental investigation of tank-type axial-flow pump device *Advances in Mechanical Engineering* **9** 168781401769568